

MATERIALS CHARACTERIZATION STUDY OF CONDUCTIVE FLEXIBLE SECOND SURFACE MIRRORS

F. Levadou and S. J. Bosma
European Space Research and Technology Centre

A. Paillous
Département d'Etudes et de Recherches en
Technologie Spatiale

SUMMARY

This paper describes the status of prequalification and qualification work being performed at ESTEC Noordwijk and at DERTS Toulouse on conductive flexible second surface mirrors.

The basic material is FEP teflon with either aluminium or silver vacuum deposited reflectors. The top layer has been made conductive by deposition of a layer of Indium oxide. Both materials have been tested in combination with a grounding method developed in the ESTEC Materials Section.

The results of a prequalification programme comprising of decontamination, humidity, thermal cycling, thermal shock and vibration tests are presented. Test parameters are thermo-optical and electrical properties. Furthermore the electrostatic behaviour of the materials under a simulated substorm environment as well as electrical conductivity at low temperatures have been characterised.

The effects of simulated ultra violet and particles irradiation on electrical and thermo-optical properties of the materials are also presented.

INTRODUCTION

In the frame of studies on electrically conductive thermal control materials, the ESTEC Materials Section has been involved since several years in the development and qualification of conductive flexible second surface mirrors (ref. 1).

The studies presented in this paper have been mainly performed for ISPM and METEOSAT projects as well as in co-operation with DERTS (Toulouse - France) on a DERTS Research Programme for evaluation of conductive thermal control materials and associated grounding techniques under simulated synchronous orbit (ref. 2, 3, 4).

This paper describes the prequalification and qualification status, as they are defined by ESTEC Materials Section, for either conductive flexible second surface mirrors (SSM) commercially available, or for commercial flexible SSM on which a conductive layer has been deposited.

The work performed by ESTEC Materials Section covers the definition and preparation of conductive materials and grounding techniques as well as the prequalification programme.

The technique for grounding conductive layers developed a few years ago by ESTEC Materials Section was utilised for these studies.

The work performed by DERTS was mainly the evaluation of the charging performance and the studies on space stability of the grounded conductive SSM under synchronous space environment.

MATERIALS PRINCIPLE

Basic materials are flexible second surface mirrors : aluminised or silvered FEP teflon and aluminised Kapton. The front face of the SSM is covered with a conductive transparent layer. The conductive layer must be transparent to avoid changes of the thermo-optical properties (i.e. absorptance and emittance) of the SSM.

The transparent conductive materials can be deposited according to different techniques and are generally Indium-oxide or Indium-Tin oxide (ITO) layers of a few hundred angström thickness.

PRINCIPLE OF THE GROUNDING CONTACT

ESTEC Materials Section has developed a few years ago a technique which can be used for grounding a conductive surface to a structural part or an intermediate metallic layer (ref. 5). The materials used for the contact joint are silicon rubber RTV 566 produced by General Electric together with conductive powder Cho-bond 1029B from Chomerics.

Preparation of the conductive adhesive

Hundred parts by weight of RTV 566A are mixed with 250 parts by weight of Cho-bond 1029B. After mixing together, the catalyst RTV 566B is added in 0.15 parts by weight. After further mixing the adhesive is degassed under vacuum.

Joint formation

Two different kind of joints have been used.

Strap joint (fig. 1)

This is an electrical contact between the conductive layer and an aluminium strap. The strap has generally dimensions of 8 mm x 80 mm and a thickness of 30 μ m. The strap is degassed by being wiped with a Kimwipe soaked in Freon TF. Then the Dow Corning DC 1200 primer is applied at the end of the strap and to the end of the conductive SSM sample. A small amount of the conductive adhesive is applied to the primed area of the conductive sample layer and the primed aluminium foil is placed over it. A special heating tool developed for this purpose by ESTEC Materials Section is applied over the joint. Cure time, temperature of the tool and load pressure are defined. Previous investigation studies have shown that ideal parameters are:

- cure time : 2 minutes
- temperature : 100°C
- load : 200 g

Blanket mode (fig. 2)

This is an electrical contact between the top conductive layer and the metallic layer (aluminium or silver/Inconel) on the back side of the SSM. A hole is punched through the sample. Primer is applied on the edges of both sides of the hole. A small amount of the conductive adhesive is put inside the hole. Two tabs of aluminium, with diameters a bit bigger than the diameter of the hole are applied on both sides of the conductive adhesive after priming. Then the heated tool is applied over the joint with the same parameters as above.

A typical application of a strap joint is at the edge of a sheet, for the interconnection of different sheets or grounding to structural elements. The blanket mode would be applied in the central part of the sheet, e.g. a thermal blanket, to connect the ITO to the metal backside of the SSM.

TEST SEQUENCE

The test sequence consists of a prequalification programme and a qualification programme as they are defined by ESTEC Materials Section Specifications.

The samples have been submitted to the following prequalification tests:

- chemical spray (also called Decontamination Test)
- humidity test
- thermal cycling test (ref. 6)
- thermal shock test
- vibration test (acoustic)

The test parameters were:

- visual inspection
- electrical contact resistance and total resistance measurements (ref. 7)
- thermo-optical properties measurements (ref. 8)
- adhesion testing (ref. 9)

Table 1 is an example of a typical prequalification programme.

Furthermore, the materials have been submitted to the following qualification tests:

- electrostatic behaviour under a simulated substorm environment
- irradiation test under UV and particles environment.

The test parameters were the same as for the prequalification tests, except that during the electrostatic test the surface potential reached by the sample has been monitored.

In annex I the method developed by ESTEC to measure both electrical contact and total resistances is described.

TEST MATERIALS

Aluminised FEP teflon with ITO deposit

- Sheldahl G409520 : 2 mil teflon thickness
- Sheldahl G409550 : 5 mil teflon thickness
- Balzers/Sheldahl : 3 mil teflon thickness with ITO deposit by Balzers.

Silver FEP teflon with ITO deposit

- Sheldahl G409420 : 2 mil teflon thickness
- Sheldahl G409450 : 5 mil teflon thickness
- General Electric/Sheldahl : 5 mil teflon thickness with ITO deposit by G.E.

Aluminised Kapton with ITO deposit

- General Electric/Sheldahl : 5 mil Kapton thickness with ITO deposit by G.E.
- Sheldahl : 0.5 mil Kapton thickness with Nomex scrim.

Table 2 shows a list of typical values for optical and electrical properties of these materials.

TEST RESULTS

Effects of chemical spray

This test is incorporated in the prequalification programme to simulate the effects of cleaning the conductive materials. Test samples are sprayed for one minute with iso-propyl-alcohol. None of the materials showed a significant variation of electrical conductivity. There is in some cases a slight improvement of solar absorptance due to the cleaning procedure.

Effects of humidity exposure

The test materials are submitted to 95% relative humidity and a temperature of 50°C during one week.

It appears that humidity has a direct influence on the conductivity of Indium oxyde or Indium-Tin oxyde layers. All test materials show considerable increases in resistivity after exposure; some typical results are:

- 5 mil silver teflon : before humidity 0.1×10^6 to $10 \times 10^6 \ \Omega$
after humidity 10^6 to $10^9 \ \Omega$
- 2 mil aluminised teflon : before humidity 5×10^6 to $20 \times 10^6 \ \Omega$
after humidity $10^8 \ \Omega$
- 0.5 mil alumin. Kapton : before humidity 1×10^6 to $20 \times 10^6 \ \Omega$
after humidity 10^7 to $10^9 \ \Omega$

After the humidity exposure several test samples were submitted to high vacuum and the electrical resistance monitored in-situ.

The conductivity of each material increased under vacuum conditions, an improvement which continued throughout the exposure to vacuum. An example is shown in fig. 3. These facts support the theory that water absorption has a degrading effect on the conductivity of Indium based layers, but that these effects are not of a permanent nature at least after short term exposure to humid conditions. There is, however, evidence that these layers will not recover after long duration exposure (2 years) to humidity levels of 70% or higher. The optical properties of the conductive SSM are not affected by the humidity test.

Effects of thermal cycling

The tests were performed in accordance with specification ESA-PSS-11 (ORM-04T). Some materials were submitted to 100 cycles between +100°C and -150°C, other materials to 100 cycles between +25°C and -150°C. Thermal cycling proved to be detrimental to teflon-based SSM for both sets of temperature limits. The ITO layer on teflon shows numerous microcracks (fig. 4), which are believed to be caused by local stresses originating from the difference in thermal expansion for teflon and ITO. In the case of silver coated teflon, the silver reflector also showed microcracking (fig. 5).

On the contrary, ITO layers on Kapton based SSM proved to be stable. No cracking was observed and the conductivity of the ITO layer improved as would be expected due to removal of absorbed water during the vacuum and temperature conditions of the thermal cycling.

Some typical results are:

- 5 mil silver teflon : before cycling 0.1×10^6 to $10 \times 10^6 \Omega$
after cycling 10^8 to $10^{10} \Omega$
- 2 mil aluminised teflon : before cycling 5×10^6 to $20 \times 10^6 \Omega$
after cycling $> 10^{10} \Omega$
- 0.5 mil alumin. Kapton : before cycling 1×10^6 to $20 \times 10^6 \Omega$
after cycling 1×10^6 to $10 \times 10^6 \Omega$

The 2 mil teflon had a "milky" appearance after cycling, which caused an increase of solar absorptance.

The cracks in the silver reflector of the 5 mil teflon SSM did not cause any measurable variation in optical properties, but are liable to cause losses due to corrosion during long term contact with chemical agents (as existing in an adhesive).

The Kapton SSM also showed no change in optical properties.

Effects of low temperature

Test configuration

The surface resistivity measurement is performed with a three electrode arrangement. This method is illustrated in Annex 2.

Test facility

The test sample with the electrode configuration was mounted to the sample holder of the "BISE" (ref. 10) vacuum facility. This sample holder is a hollow disc through which it is possible to circulate liquid nitrogen.

The temperature of the sample was monitored with three chromel-alumel thermocouples. The electrical leads of the electrode configuration were connected to an electrical vacuum feedthrough to allow for in-situ resistance measurement. A vacuum of more than 10^{-6} torr was achieved with a turbo pump assembly. The liquid nitrogen shroud of the "BISE" chamber was filled before cooling down the sample to avoid excess contamination depositing on the cooled sample surface.

Electrical measurement method

In-situ measurement: The Voltmeter method was applied, as illustrated in the electrical diagram of fig. 6. The internal resistance of the electrometer is connected in serie with the unknown resistance, to serve as a current limiting element. The current to the test sample was set at 1×10^{-6} A and applied continuously during the test. Voltage and temperature over the test sample were measured and monitored with a chart-recorder during the test run.

Ex-situ measurement: The surface resistivity (ρ_s) has been measured with a probe consisting of two 1 cm wide copper electrodes at 1 cm distance of each other, in combination with a Hewlett Packard digital multimeter 3456B. A weight of 200 g was applied to maintain a standard pressure on the probe. Readings are made after one minute electrification time.

Sample conditioning

The sheet material is stored under a relative humidity of 65% - 70% and a temperature of 18°C - 20°C.

Ex-situ measurements of surface resistivity are performed in the conditions stated above.

In-situ measurements of surface resistivity are performed in the prevailing chamber conditions.

Test results

Table 3 compiles the last results for the SSM materials. Although the samples do not have similar "absolute" results, they behave identical in various ways:

- Three out of four samples show a sudden decrease in surface resistivity after first exposure to vacuum.
- All samples show a significant drop in surface resistivity after the total test phase, when compared to the initial value under identical conditions.
- All samples show an increase in surface resistivity after air inlet.
- All samples show a drop in surface resistivity when irradiated with UV light and subsequent recovery after interruption of the UV radiation.
- All samples show an increase in surface resistivity with temperature decrease. A nominal value is difficult to determine but it appears that the rate of change is related to the absolute value of surface resistivity of the sample. In terms of the final ρ_s in vacuum, the $\Delta\rho_s/\Delta T$ varies between 1% and 10% of ρ_s .
- Water absorption has a highly negative effect on the conductivity of ITO. The tests demonstrate that the conductivity of the ITO layer improves with vacuum exposure time (fig. 3).

Fig. 7 shows a typical curve for surface resistivity as a function of temperature. The lower two curves are the cooling down and warming-up phases with no correction for the vacuum recovery effects. The upper two curves have been corrected for this phenomenon.

Effects of electrostatic testing

In order to assess the electrostatic behaviour of ITO coated SSMs, various samples have been tested at DERTS in the CEDRE simulation chamber.

This facility enables to irradiate specimens with electrons in the 4-25 keV range. The irradiation uniformity (better than 10 percent) at the sample is obtained by scattering of the electrons through a thin aluminium foil (1.2 μm thick). Samples are maintained in close contact by their rear side with an aluminium plate which is grounded through a nanoammeter which enables to measure the leakage current I during irradiation. The current I_{sec} collected on a hemicylindrical electrode surrounding the sample allows to evaluate the secondary emission of the irradiated surface. The conductive ITO layer is grounded by means of either a metallic frame in contact with the surface or aluminium straps bonded to the ITO by conductive adhesive, which enables to measure the surface leakage current I_{surf} .

The surface potential of the specimens is measured by a contactless method with a potential probe (capacitive sensor) moved by a mechanical scanner. Impulses in the recording of the leakage current indicate the occurrence of discharges if any.

Table 4 shows that the ITO layers deposited by BALZERS and SHELDAHL are equally effective in suppressing potential build up and discharges, when grounded. The surface potentials of non-coated SSMs are also given in table 4 as a comparison. No potential increase has been identified after that both ITO coated samples had been rolled around cylinders (4 mm diameter) in perpendicular directions.

Table 5 gives the results that have been measured under irradiation on two ITO coated aluminised Kapton samples, of which the ITO layer was grounded by means of four interconnects obtained by the conductive adhesive technique; one of these samples has undergone all the prequalification tests. No charge build up has been noticed in the simulated substorm environment. However, the secondary emission as well as the leakage current seem slightly higher in the case of the sample exposed to the prequalification programme. However, its total surface current (collected by the aluminium straps bonded to the ITO) is still very high.

Effects of simulated space irradiation

The stability of various conductive SSM has been assessed by irradiation either with UV only or with UV and particles.

Figure 8 gives the results of an irradiation by UV of ITO layers applied by SHELDAHL on silvered FEP 2 and 5 mil thick. The degradation under UV of a 3 mil aluminised FEP from SHELDAHL is also reported in figure 8 together with the degradation of the same aluminised film that has been coated by an ITO layer made by BALZERS. The solar reflectance variations have been obtained at DERTS from in-situ spectral measurements that have been carried out on samples irradiated at 30°C under vacuum by two filtered Xenon short arc sources giving only ultra-violet radiation in the 200-380 nm wavelength range with a sun multiplication factor of 2.

The same UV sources have also been used in conjunction with proton and electron accelerators in order to provide conditions of exposure simulating the geosynchronous orbit environment for a North/South satellite face. The irradiation was sequential with a continuous ultra-violet exposure (2 "suns") and periodic particle bombardment.

In order to simulate one year in space, the following conditions were chosen 1112 UV esh, 4.29×10^{14} protons cm^{-2} at 40 keV (normal incidence), 1.42×10^{13} protons cm^{-2} at 150 keV (normal incidence), 8.6×10^{14} electrons cm^{-2} (45° incidence). Figure 8 shows the solar reflectance variations that have been measured on a silvered FEP sample (2 mil) and a silvered FEP sample (2 mil thick) with an ITO layer deposited by SHELDAHL. During irradiations the ITO layers were grounded. From the curves in figure 8, it seems that the degradation kinetics of the conductive ITO manufactured by SHELDAHL and irradiated by UV plus particles is nearly identical with the one observed as consequence of an irradiation by UV only. That means that UV radiation is more deleterious than particles in optical degradation of ITO layers. In spite of the short duration of the tests, a tendency towards saturation is noted in the degradation of these conductive layers. On the other hand, the second surface mirrors without conductive overcoating are more severely degraded when irradiated simultaneously by particles and ultra-violet. Of significance might be the less extent of degradation observed in figure 8 with the ITO coatings made by BALZERS and GENERAL ELECTRIC: the preparation method is of prime importance in the colour centre formation under radiation. The behaviour of the ITO layer is the same whether it is grounded during particle irradiation or not.

It has been verified that the total electrical resistance measured in-situ between aluminium straps applied with conductive RTV 566 on the ITO layers (2 mil silvered FEP SHELDAHL) was not modified by exposure to the combined environment described above. (N.B. the samples were not illuminated nor irradiated by particles during measurements).

DISCUSSION

This research programme has established that conductive layers of Indium-oxide or Indium-tin-oxide do not have a general behaviour pattern, but depend on different application parameters. The performance of the conductive layer will vary with such factors as:

- deposition technique (e.g. vapour deposition or sputtering)
- substrate material
- substrate temperature during deposition
- random conditions during deposition (vacuum, contamination)
- material history (perforation, humidity exposure, handling)

Of the flexible materials tested, Kapton proved to be the best host for an Indium based conductive layer.

Two prequalification programmes on two individual materials from different manufacturers showed that the ITO layer is mechanically stable: no cracks were observed after thermal cycling, neither for a vapour deposited layer nor a sputtered layer. The initial electrical and optical properties did not show major variations after the total prequalification. The conductivity of the ITO layer recovered during thermal cycling from water absorbed during the humidity test. No significant charge build up was observed on the sputtered layer during the electrostatic charging test either on the original material or on a sample which had undergone all prequalification tests.

Teflon based conductive SSM proved to be extremely vulnerable to thermal cycling: both sputtered and vapour deposited ITO layers showed numerous microcracks. In the case of the silver SSM, the metal reflector was also cracked. Thermal cycling caused the 2 mil aluminised teflon to go milky which resulted in a degradation of solar absorptance. The initial resistivity of teflon based conductive SSM tends to be higher than the equivalent Kapton material. The teflon based SSM does not charge during electrostatic charging tests, however, recent results show that a sample which had been submitted to the total prequalification programme did support charge up to several hundred volts.

The degradation of the optical properties of ITO layers under simulated irradiation is very dependant on deposition type and manufacturer. Based on UV and particle irradiation sputtered ITO (GENERAL ELECTRIC) appears to be more stable than vapour deposited ITO (SHELDAHL). The main degrading factor is ultra-violet irradiation, although BALZERS vapour deposit an ITO layer which is very stable under ultra-violet exposure. Unfortunately this material is a one time experimental batch made by BALZERS under ESA contract and is not commercially available. The degradation of the ITO due to UV has a tendency to saturate after exposure periods of more than a year.

Indium based conductive layers are very vulnerable to water absorption. Short term humidity effects will recover during vacuum exposure, however, long term humidity effects cause permanent damage. It is recommended to store conductive SSM in a controlled dry environment and to record batch histories with respect to storage conditions and handling.

The ESA developed grounding technique based on conductively loaded RTV 566 proved to be applicable on both Kapton and teflon SSM and was stable during prequalification and qualification tests.

CONCLUSIONS

Kapton based SSM with a conductive ITO layer is a very promising solution for electrostatic charging problems. The teflon based SSM with a conductive ITO layer evaluated during this programme will not fulfil strict electrostatic charging requirements. There are still a number of verification tests on-going to determine if the present material, despite the risk of ITO cracking could be used on spacecraft which can tolerate limited charging levels.

Manufacturers are recommended to investigate the possibilities of optimising the ITO layers on teflon with respect to deposition technique, substrate temperature etc. This test programme indicates that initial optical and electrical properties as well as space stability depend heavily on these factors.

Manufacturers must be able to guarantee an ITO layer of standard quality if this type of solution is to be competitive with other types of conductive thermal control coatings in the future.

REFERENCES

1. Bosma, J. and Levadou F.; Electrostatic Charging and Space Materials. ESA SP-145, October 1979.
2. Paillous, A.; Revêtements Conducteurs Envisagés pour le Satellite METEOSAT. Etude CERT 4108. Contrat ESTEC 4294/80/NL/PP, July 1980.
3. Benisja, A., Levy L., Paillous, A. and Sarrail, D.; Satellite Spacecraft Charging Control Materials. Interim Scientific Report No. 1. Grant Number AFOIR 78-3704B, July 1979.
4. Levy, L., Paillous, A. and Sarrail, D.; Satellite Spacecraft Charging Control Materials. Interim Scientific Report No. 2. Grant Number AFOIR 78-3704B.
5. Bosma, J. and Froggatt, M.; Evaluation of a Conduction Adhesive System for the Grounding of Aluminised Kapton Coated with Indium/Tin oxide, ESA STM-13, August 1980.
6. Screening Test Method for the Selection of Space Materials and Small Assembly by Thermal Cycling under Vacuum. PSS-11/QRM-04T.
7. Electrical Properties Measurements on Conductive Surfaces for Space Use. QRM-38T.
8. Specification for the Measurements of the Thermo-Optical Properties of Thermal Control Materials at ESTEC. PSS-16/QRM-09T, ESA specification.
9. Testing the Peel or Pull-Off strength of Coatings and Finishes by Means of Pressure Sensitive Tape. PSS-18/QRM-13T, ESA specification.
10. Minier, C.F.; Description du Banc d'Irradiations Solaires de l'ESTEC BISE. Internal ESTEC Working Paper No. 986.
11. Paillous, A. and Sarrail, D.; Compte Rendu Final sur Contrat ESTEC 3184/77/NL/HP. Publ. ONERA/CERT/DERTS 4064, February 1979.

ANNEX 1

ELECTRICAL RESISTANCE MEASUREMENTS

Background

In the case of a grounding point on a highly conductive substrate material, e.g. aluminium, it is sufficient to measure the total resistance of the grounding point and substrate, because a change in the contact resistance from the 10Ω range to the 100Ω range will be easily detected, the substrate resistance being a few milliohms only.

In the case of a low-ohmic contact (10Ω to 100Ω range) on a substrate material with a high ohmic resistivity ($k\Omega$ - $M\Omega$ range), the contact resistance is more difficult to determine. This is the situation for the grounding configuration under evaluation.

The Indium-Tin oxide layer shows variations of hundreds of ohms during a measurement. This is only a few tenths of one percent with respect to the actual resistance of several megohms, but is of the same order of magnitude as the contact resistance of the grounding point.

For this particular grounding configuration, the contact resistance will be defined as the combined resistances of the aluminium strap, the conductive adhesive and the ITO boundary layer at the contact point.

Electrical contact resistance

Several methods have been evaluated which appeared capable of determining the contact resistance in a high ohmic chain. Figure 1 shows the sample configuration for the method which proved to be most effective. The three-contact principle is used to obtain the contact resistance of the centre electrode. The three electrodes were formed by aluminium straps bonded with conductive adhesive, as described in section 3. Figure 1 shows the electrical circuit applied.

The power supply and the ammeter are connected to the centre and right electrodes; the right electrode functions only as a current conductor.

The voltmeter is connected between the centre and left electrodes. The left electrode functions as a potential electrode. Owing to the internal resistance of the voltmeter, the current passing through circuit "A" will be approximately a factor 1000 smaller than that passing through circuit "B".

Adjusting the power supply in circuit "B" enables the current through the contact resistance to be fixed. Circuit "A" is used to determine the voltage drop over the contact resistance, from which the contact resistance can be deduced.

On the basis of this method, a jig has been developed which ensures that the samples are measured under similar conditions of electrode pressure and sample positioning.

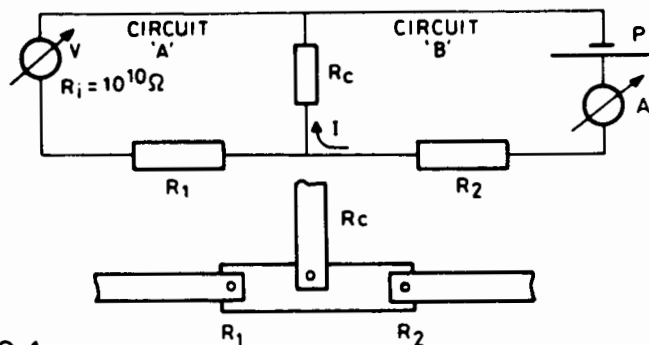


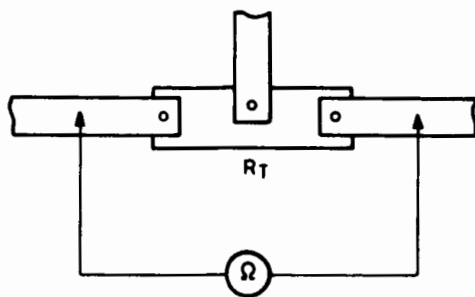
FIG. 1

The symbols used in Figure 1 have the following meanings:

- P = power supply,
- A = Keithly Model 602 electrometer (applied in ammeter mode),
- V = Hewlett Packard multimeter 3465B (applied in voltmeter mode),
- R_i = internal resistance of voltmeter = $10^{10} \Omega$,
- R_1 = contact resistance of left electrode plus resistance of ITO layer between left and centre electrodes,
- R_2 = contact resistance of right electrode plus resistance of ITO layer between right and centre electrodes,
- R_c = contact resistance of centre electrode.

Total electrical resistance

After each successive test, the total electrical resistance of each sample was measured with the Hewlett Packard multimeter 3465B applied in ohmmeter mode. The total electrical resistance is defined as the electrical resistance measured between left and right electrodes and includes contact resistance of left and right electrodes as well as the resistance of the intervening ITO layer. Figure 2 illustrates the test method.



Ω = OHMMETER
 R_T = TOTAL ELECTRICAL RESISTANCE

FIG. 2

ANNEX 2

SURFACE RESISTIVITY MEASUREMENT

We now consider a strip of width dx which is at a radius x from the centre of the sample. The resistance of the strip according to the definition of the surface resistivity is:

$$dR = \rho_s \times dx / 2\pi x \quad (1)$$

ρ_s = surface resistivity (Ohm).

The voltage drop dV over this section will be:

$$dV = I \times dR \quad (2)$$

I = current through sample,

$$\text{or} \quad dV = I \times \rho_s \times dx / 2\pi x \quad (3)$$

The total voltage drop between two electrodes of radius R_1 and R_2 will be:

$$\int_{V_1}^{V_2} dV = \rho_s \times I \int_{R_1}^{R_2} \frac{dx}{2\pi x} \quad (4)$$

$$V_2 - V_1 = \frac{\rho_s \times I}{2\pi} \ln \frac{R_2}{R_1} \quad (5)$$

The surface resistivity between two electrodes is given by:

$$\rho_s = 2\pi V / I \times \ln \frac{R_2}{R_1} \quad (6)$$

For the dimensions of the two inner electrodes as shown in fig. 1 the equation is:

$$\rho_s = 2\pi (V/I) / \ln \frac{67}{50} \quad (7)$$

$$\rho_s = 21.47 \frac{V}{I} \quad (8)$$

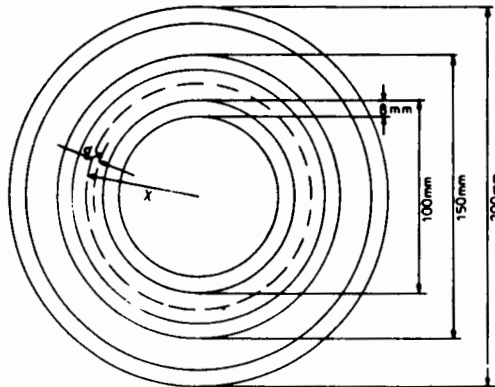


FIG 1 ELECTRODE CONFIGURATION

Material	α_s	ϵ_N	ρ_s
Sheldahl alu teflon 2 mil	0.18	0.64	6-19 M Ω
Sheldahl alu teflon 5 mil	0.20	0.76	9-40 M Ω
Balzers alu teflon 3 mil	0.15-0.17	0.71	0.5-2 K Ω
Sheldahl Ag teflon 2 mil	0.08-0.09	0.64	0.8-2 M Ω
Sheldahl Ag teflon 5 mil	0.10	0.77	1-2 M Ω
G.E. Ag teflon 5 mil	0.12-0.16	0.79-0.80	1-20 M Ω
G.E. alu kapton 5 mil	0.38-0.39	0.77	60-140 K Ω
Sheldahl alu kapton 0.5 mil	0.75-0.73	0.48	50-260 K Ω

Table 2 - Materials Properties

Material	Initial ρ_s in air R.T.	Initial ρ_s in vacuum R.T.	$\Delta\rho_s/\Delta T$	Final ρ_s in vacuum R.T.	ρ_s after UV	Final ρ_s in air R.T.
SHELDAHL FEP/AL 2 mil	22 M Ω	24 M Ω	113-117 K Ω /°C	6 M Ω	4.6 M Ω	9.4 M Ω
SHELDAHL FEP/Al 5 mil	20 M Ω	7 M Ω	0.60 M Ω /°C	6 M Ω	3.0 M Ω	11.4 M Ω
SHELDAHL FEP/Ag 5 mil	8 M Ω	7 M Ω	104-118 K Ω /°C	2 M Ω	0.9 M Ω	1.2 M Ω
BALZERS FEP/Al 3 mil	9.0 K Ω	7.6 K Ω	34-43 Ω /°C	3.2 K Ω	2.6 K Ω	5.8 K Ω

Table 3

BEAM ENERGY (keV)	INTENSITY (nA cm ⁻²)	SURFACE POTENTIAL VOLTS			
		ALUMINIZED FEP 3 mil	ITO (BALZERS) on Aluminised FEP 3 mil	SILVERED FEP 2 mil	ITO (SHELDAHL) on Silvered FEP 2 mil
5	1	1900	< 10	2000	< 10
10	1	5400	< 10	5400	< 10
15	1	10300	< 10	10000	< 10
20	1	15000	< 10	15000	< 10
25	1	discharges	< 10	9800	< 10
10	5	5500	< 10	5400	< 10
15	5	10300	< 10	10000	< 10
20	5	15400	< 10	15400	< 10

Table 4 - Behaviour of ITO coated FEP in a simulated substorm environment. (Not submitted to prequalification test).

		BEAM ENERGY/INTENSITY			
		5 keV	10 keV	15 keV	20 keV
		1.25 nA cm ⁻²	0.7 nA cm ⁻²	0.5 nA cm ⁻²	0.5 nA cm ⁻²
BEFORE PREQUALIFICATION PROGRAM	V (volts)	< 10	< 10	< 10	< 10
	I (nA)	0.5	0.2	0.08	0.12
	I _{surf} (nA)	10.5	11.5	11	10.5
	I _{sec} (nA)	12	4	2.5	1.5
	Discharges	no	no	no	no
AFTER PREQUALIFICATION PROGRAM	V (volts)	< 10	< 10	< 10	< 10
	I _c + I _L (nA)	1	1.1	1.2	1.2
	I _{surf} (nA)	4	5.5	9	8
	I _{sec} (nA)	16	8	2.5	1.7
	Discharges	no	no	no	no

TABLE 5 - BEHAVIOUR OF THE ITO-COATED KAPTON GROUNDED WITH A CONDUCTIVE ADHESIVE IN A SIMULATED SUBSTORM ENVIRONMENT

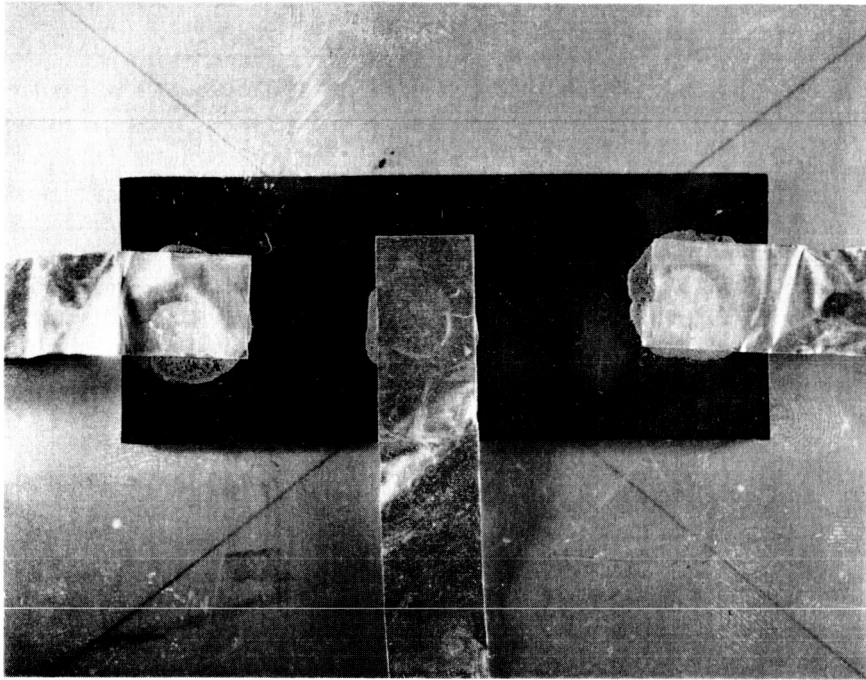


FIG. 1: GROUNDING STRAP CONFIGURATION

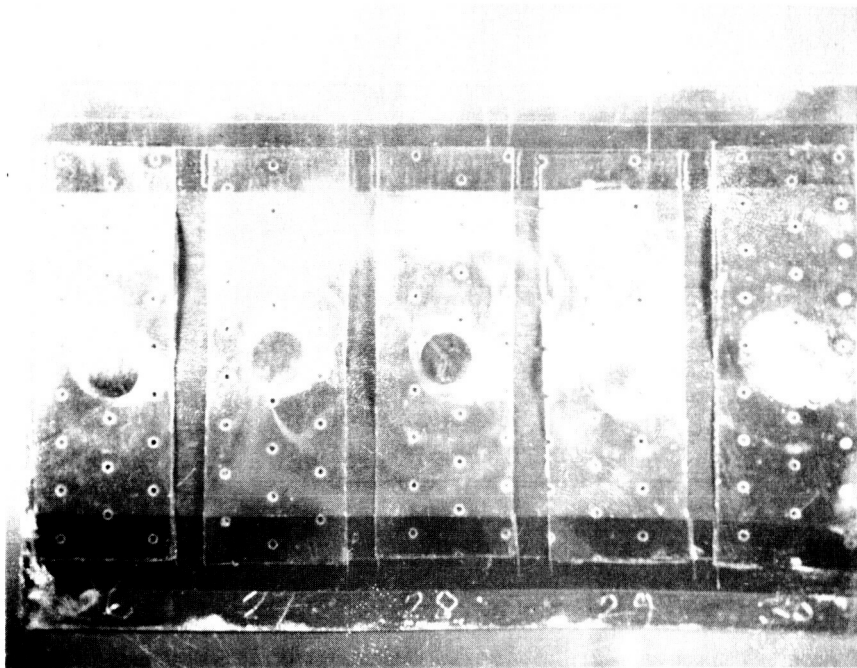


FIG. 2: BLANKET MODE GROUNDING CONFIGURATION

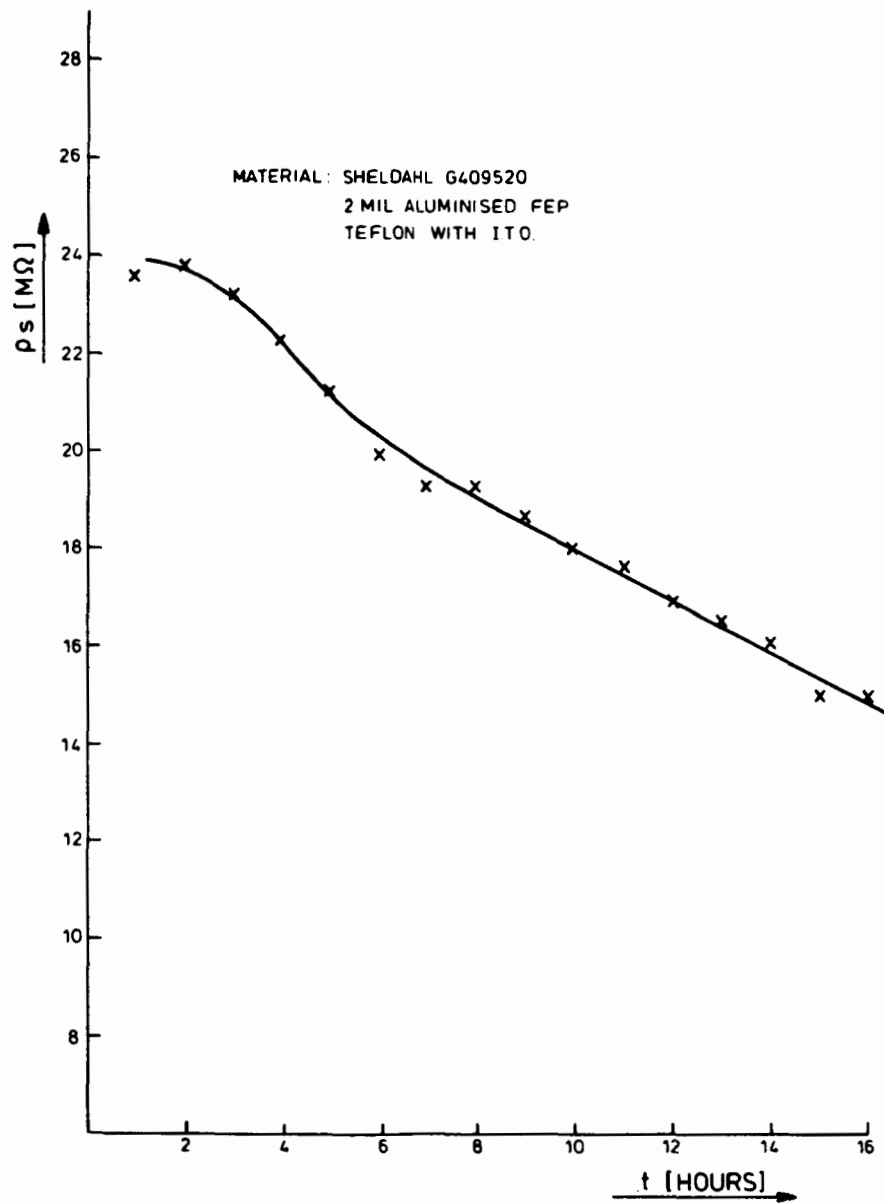


FIG.3 SURFACE RESISTIVITY AS A FUNCTION OF TIME

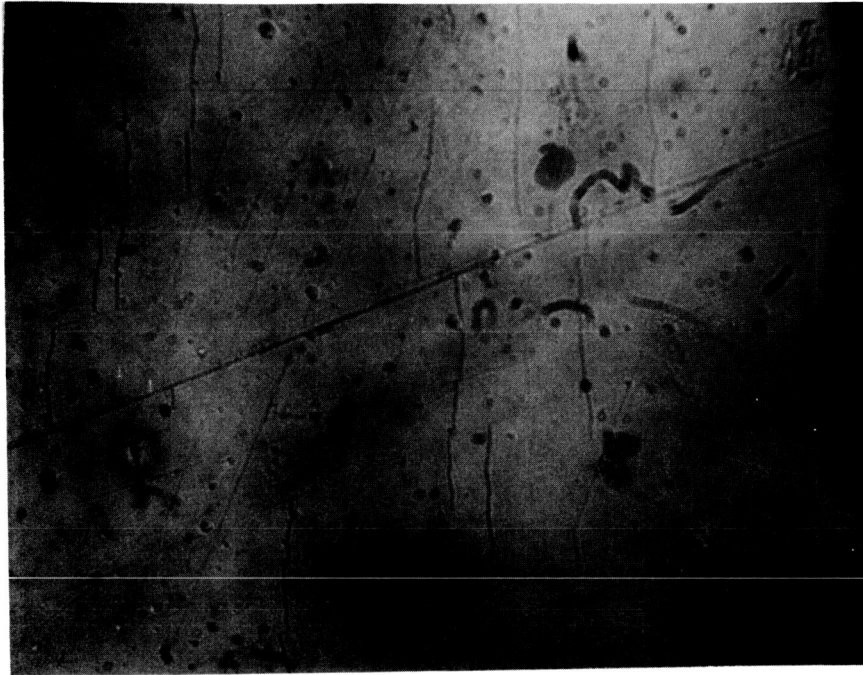


Fig. 4: Micro-cracks in I.T.O.-layer after thermal cycling.

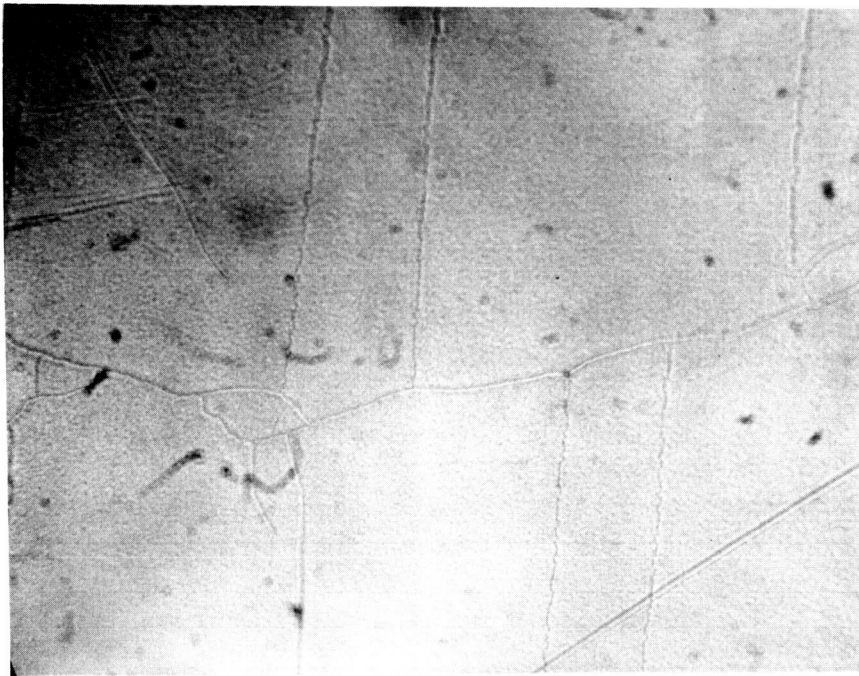


Fig. 5: Micro-cracks in silver layer after thermal cycling.

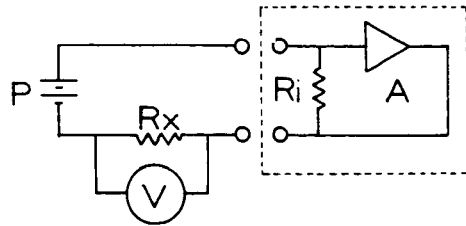


Fig. 6 Electrical measurement diagram.

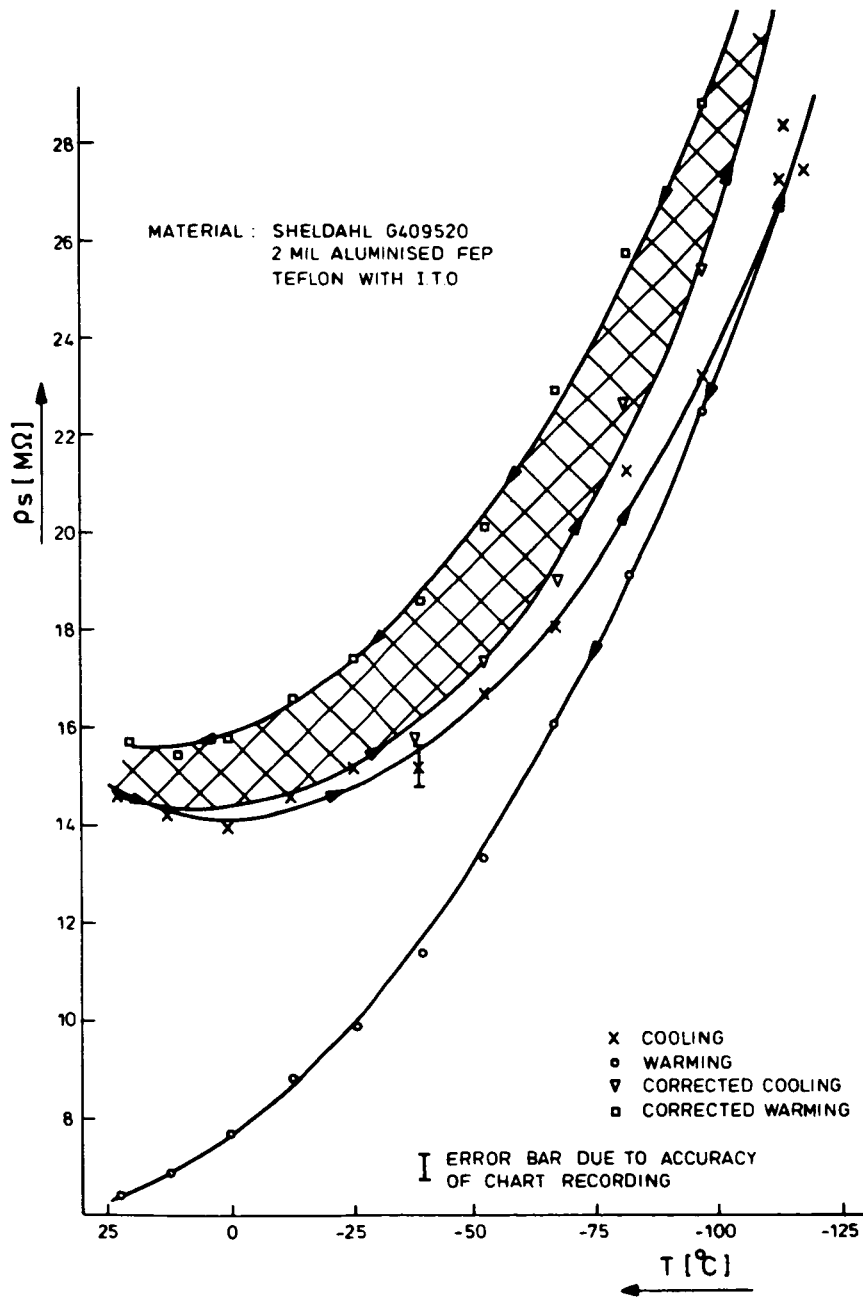


FIG.7 SURFACE RESISTIVITY AS A FUNCTION OF TEMPERATURE

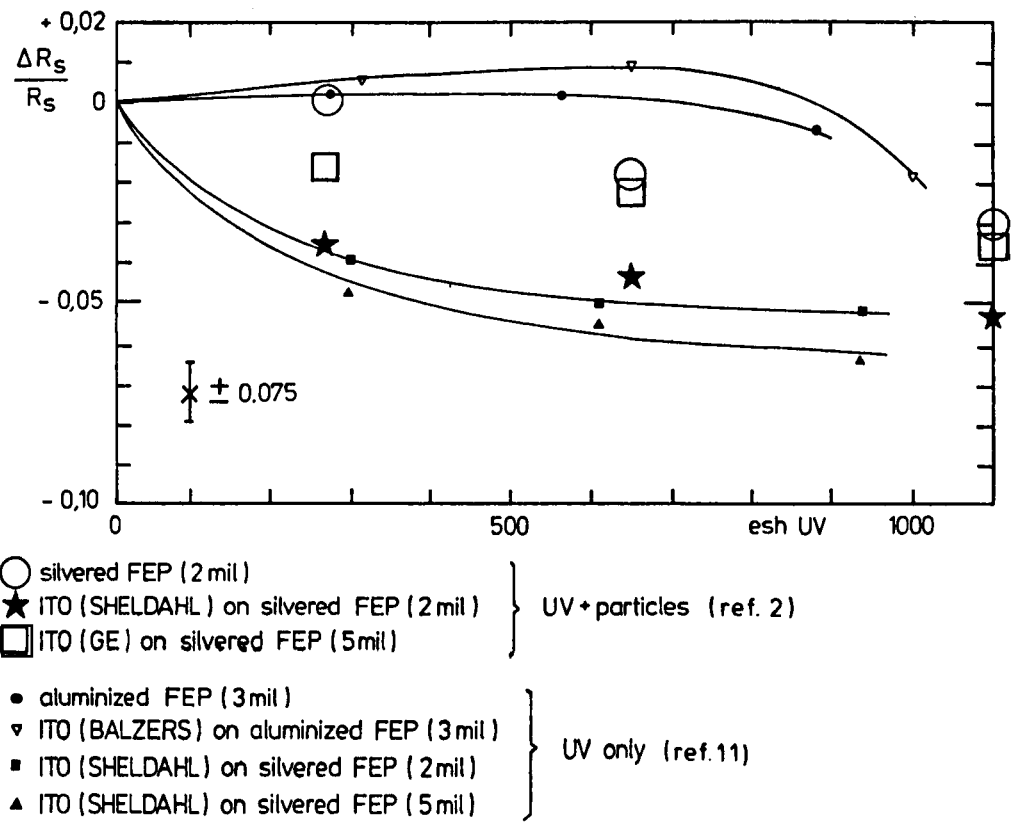


FIG.8